Full quantum state reconstruction of symmetric two-mode squeezed thermal states via spectral homodyne detection and a state-balancing detector

Simone Cialdi,[1,2] Carmen Porto,[1] Daniele Cipriani,[1] Stefano Olivares,[1,2] and Matteo G. A. Paris[1,2]
[1]*Dipartimento di Fisica, Università degli Studi di Milano, I-20133 Milano, Italy*
[2]*Istituto Nazionale di Fisica Nucleare, Sezione di Milano, Via Celoria 16, I-20133 Milan, Italy*
(Received 18 May 2015; published 5 April 2016)

We suggest and demonstrate a scheme to reconstruct the symmetric two-mode squeezed thermal states of spectral sideband modes from an optical parametric oscillator. The method is based on both a single homodyne detector and the error signal from the active stabilization of the oscillator cavity. The measurement scheme has been successfully tested on different two-mode squeezed thermal states, ranging from uncorrelated coherent states to entangled states.

DOI: 10.1103/PhysRevA.93.043805

I. INTRODUCTION

Homodyne detection (HD) is an effective tool to characterize the quantum state of light in either the time [1–8] or the frequency [9–28] domain. In a spectral homodyne detector, the signal under investigation interferes at a balanced beam splitter with a local oscillator (LO) with frequency ω_0. The two outputs undergo a photodetection process and their photocurrents are combined leading to a photocurrent continuously varying in time. The information about the spectral field modes at frequencies $\omega_0 \pm \Omega$ (sidebands) is then retrieved by electronically mixing the photocurrent with a reference signal with frequency Ω and phase Ψ. Upon varying the phase θ of the LO, we may access different field quadratures, whereas the phase Ψ can be adjusted to select the symmetric $\mathscr{S}$ or antisymmetric $\mathscr{A}$ balanced combinations of the upper and lower sideband modes.

Measuring the sole modes $\mathscr{S}$ and $\mathscr{A}$ through homodyne detection is not enough to assess the spectral correlation between the modes under investigation [29] and, in turn, to fully characterize a generic quantum state. In order to retrieve the full information about the sidebands it has been suggested that one should spatially separate the two modes [30,31] or implement more sophisticated setups [29,32] involving resonator detection. On the other hand, it would be desirable to have schemes that do not require structural modifications of the experimental setup. In turn, this would make it possible to embed more easily diagnostic tools in interferometry [33] and continuous-variable-based quantum technology. Remarkably, in many relevant cases of interest for continuous-variable quantum information, such as squeezed state generation by spontaneous parametric down-conversion, the correlation between the modes vanishes due to the symmetric nature of the generated state, which should be, of course, experimentally verified.

In this paper we focus on the characterization of a signal from an optical parametric oscillator (OPO) that is the main source of continuous-variable quantum states exploited in quantum-information processing protocols. We suggest and demonstrate a measurement scheme where the relevant information for the quantum state reconstruction of symmetric spectral modes is obtained by using both a single homodyne detector and the error signal of an active stabilizer. The latter is based on the Pound-Drever-Hall (PDH) technique [34] and stabilizes an OPO used for the state generation. More precisely, we use the error signal from the PDH to stabilize the OPO as well as to monitor the state balance. Furthermore, the reconstruction is achieved by exploiting the phase coherence of the setup, guaranteed in every step of the experiment, and two auxiliary combinations of the sideband modes selected by setting the mixer phase at $\Psi = \pm\pi/4$.

The paper is structured as follows. In Sec. II we describe the state generation and the homodyne detection technique. Section III presents the obtained results concerning coherent, squeezed, and squeezed-coherent two-mode states. We draw some concluding remark in Sec. IV.

II. HOMODYNE DETECTION AND STATE RECONSTRUCTION

A. Experimental setup

A schematic diagram of our apparatus is sketched in Fig. 1. The principal radiation source is provided by a home-made Nd:YAG laser (∼300 mW @1064 and 532 nm) internally frequency doubled by a periodically poled MgO:$LiNbO_3$ (PPLN in Fig. 1). To obtain the single-mode operation, a light diode is placed inside the laser cavity. One laser output (@532 nm) pumps the MgO:$LiNbO_3$ crystal of the OPO whereas the other output (@1064 nm) is sent to a polarizing beam splitter (PBS) to generate the LO and the seed for the OPO. The power of the LO (∼10 mW) is set by an amplitude modulator (AM). Two phase modulators (PMa and PMb in Fig. 1) generate both the sidebands used as OPO coherent seeds and as active stabilization of the OPO cavity with the PDH technique [34]. For the OPO stabilization we use a frequency of 110 MHz (HF) while the frequency $\Omega/(2\pi)$ for the generation of the input seed is about 3 MHz. This is indeed a major effort, but it will turn out to be fundamental for the *full* reconstruction of the symmetric states addressed below. The OPO cavity is linear with a free spectral range (FSR) of 3300 MHz, the output mirror has a reflectivity of 92% and the rear mirror of 99%. The linewidth is about 55 MHz, thus the OPO stabilization frequency HF is well above the OPO linewidth while the frequency Ω is well inside. In order to actively control the length of the OPO cavity its rear mirror is connected to a piezo that is controlled by the signal error of the PDH apparatus.

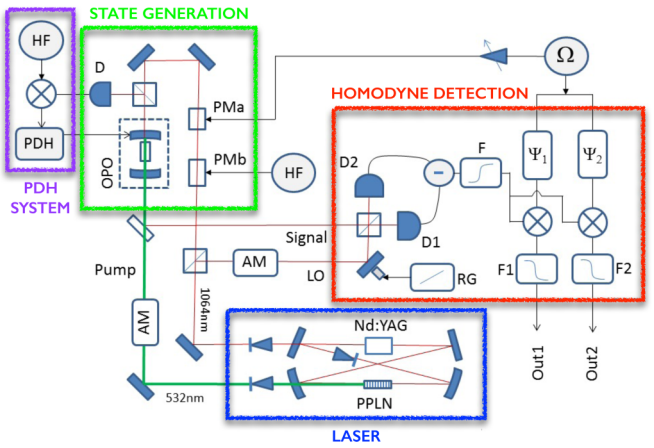

FIG. 1. Schematic diagram of the experimental setup. See the main text for details.

The detector consists of a 50:50 beam splitter, two low-noise detectors and a differential amplifier based on a LMH6624 operational amplifier. The interferometer visibility is about 95%. We remove the low-frequency signal through a high-pass filter @500 kHz and then the signal is sent to the demodulation stage. To extract the information about the signal at frequency Ω we use an electronic setup consisting of a phase shifter, a mixer ($\otimes$ in Fig. 1), and a low-pass filter @300 kHz. Since, as we will see in the following, we need to measure the signal at two different orthogonal phases, Ψ_1 and $\Psi_2 = \Psi_1 + \pi/2$, for the sake of simplicity we implemented a double electronic setup to observe the outputs at the same time (see Fig. 1). Finally, the LO phase θ is scanned between 0 and 2π by a piezo driven by a ramp generator (RG) and connected with a mirror before the HD beam splitter. The acquisition time is 20 ms and we collect about 100 000 points by a 2-GHz oscilloscope.

B. OPO state reconstruction protocol

If $\tilde{a}_0(\omega_0)$ is the photon annihilation operator of the signal mode at the input of the HD, it is easy to show that the detected photocurrent can be written as (note that the "fast term" ω_0 is canceled by the presence of the LO at the same frequency) $I(t) \propto \tilde{a}_0(t)\, e^{-i\theta} + \tilde{a}_0^\dagger(t)\, e^{i\theta}$ [35], where θ is the phase difference between the signal and LO and we introduced the time-dependent field operator $\tilde{a}_0(t)$, which is slowly varying with respect to the carrier at ω_0, such that $\tilde{a}_0(t) = e^{-i\omega_0 t} \int d\omega\, F(\omega)\, \tilde{a}_0(\omega_0+\omega)\, e^{-i\omega t} \equiv e^{-i\omega_0 t} a_0(t)$, $F(\omega)$ being the apparatus spectral response function.

To retrieve the information about the sidebands at frequencies $\omega_0 \pm \Omega$, described by the time-dependent field operators $a_{\pm\Omega}(t)$, we use electronic mixers set at the frequency Ω with phase shift Ψ with respect to the signal, leading to the current $I_\Omega(t,\Psi) = I(t)\cos(\Omega t + \Psi)$. Neglecting the terms proportional to $\exp(\pm 2i\Omega t)$ (low-pass filter), we find the following expression for the operator describing the (spectral) photocurrent $I_\Omega(t,\Psi) \propto X_\theta(t,\Psi|\Omega)$, where $X_\theta(t,\Psi|\Omega) = b(t,\Psi|\Omega)\, e^{-i\theta} + b^\dagger(t,\Psi|\Omega)\, e^{i\theta}$ is the quadrature operator associated with the field operator (note the dependence on the two sidebands):

$$b(t,\Psi|\Omega) = \frac{a_{+\Omega}(t)\, e^{i\Psi} + a_{-\Omega}(t)\, e^{-i\Psi}}{\sqrt{2}}. \tag{1}$$

Note that $[b(t,\Psi|\Omega), b^\dagger(t',\Psi|\Omega)] = \int d\omega\, |F(\omega)|^2\, e^{-i\omega(t-t')}$.

The interaction inside the OPO is bilinear and involves the sideband modes $a_{\pm\Omega}$ [35]. It is described by the effective Hamiltonian $H_\Omega \propto a_{+\Omega}^\dagger a_{-\Omega}^\dagger + \text{H.c.}$, which is a two-mode squeezing interaction. Due to the linearity of H_Ω, if the initial state is a coherent state or the vacuum, the generated two-mode state ρ_Ω is a Gaussian state, namely, a state described by Gaussian Wigner functions and, thus, fully characterized by its covariance matrix (CM) $\boldsymbol{\sigma}_\Omega$ and first moment vector $\boldsymbol{R}$ [36,37]. It is worth noting that due to the symmetry of H_Ω, the two-sideband state is symmetric [29] and can be written as $\rho_\Omega = D_2(\alpha)S_2(\xi)\nu_{+\Omega}(N) \otimes \nu_{-\Omega}(N)S_2^\dagger(\xi)D_2^\dagger(\alpha)$, where $D_2(\alpha) = \exp\{[\alpha(a_{+\Omega}^\dagger + a_{-\Omega}^\dagger) - \text{H.c.}]/\sqrt{2}\}$ is the symmetric displacement operator and $S_2(\alpha) = \exp(\xi a_{+\Omega}^\dagger a_{-\Omega}^\dagger - \text{H.c.})$ the two-mode squeezing operator, and $\nu_{\pm\Omega}(N)$ is the thermal state of mode $a_{\pm\Omega}$ with N average photons [36]. The state ρ_Ω belongs to the so-called class of the two-mode squeezed thermal states, generated by the application of $S_2^\dagger(\xi)D_2^\dagger(\alpha)$ to two thermal states with (in general) different energies. In order to test our experimental setup, we acted on the OPO pump and on the phase modulation to generate and characterize three classes of states: the coherent ($\alpha \neq 0$ and $N,\xi = 0$), the squeezed ($\xi, N \neq 0$ and $\alpha = 0$), and the squeezed-coherent ($\alpha,\xi,N \neq 0$) two-mode sideband states. We now consider the mode operators

$$b(t,0|\Omega) \equiv a_\text{s}, \quad b(t,\pi/2|\Omega) \equiv a_\text{a}, \tag{2}$$

which correspond to the symmetric ($\mathscr{S}$) and antisymmetric ($\mathscr{A}$) combination of the sideband modes, respectively, and the corresponding quadrature operators $q_k = X_0(t,\Psi_k|\Omega)$, $p_k = X_{\pi/2}(t,\Psi_k|\Omega)$, and $z_k^\pm = X_{\pm\pi/4}(t,\Psi_k|\Omega)$, $k = \text{a,s}$, with $\Psi_\text{s} = 0$ and $\Psi_\text{a} = \pi/2$. In the $\mathscr{S}/\mathscr{A}$ modal basis, the first moment vector of ρ_Ω reads $\boldsymbol{R}' = (\langle q_\text{s}\rangle, \langle p_\text{s}\rangle, \langle q_\text{a}\rangle, \langle p_\text{a}\rangle)^T$ and its 4×4 CM can be written in the following block-matrix form:

$$\boldsymbol{\sigma}' = \begin{pmatrix} \boldsymbol{\sigma}_\text{s} & \boldsymbol{\sigma}_\delta \\ \boldsymbol{\sigma}_\delta^T & \boldsymbol{\sigma}_\text{a} \end{pmatrix}, \quad \boldsymbol{\sigma}_\delta = \begin{pmatrix} \varepsilon_q & \delta_{qp} \\ \delta_{pq} & \varepsilon_p \end{pmatrix}, \tag{3}$$

where [38]

$$\boldsymbol{\sigma}_k = \begin{pmatrix} \langle q_k^2\rangle - \langle q_k\rangle^2 & \frac{1}{2}\langle (z_k^+)^2 - (z_k^-)^2\rangle \\ \frac{1}{2}\langle (z_k^+)^2 - (z_k^-)^2\rangle & \langle p_k^2\rangle - \langle p_k\rangle^2 \end{pmatrix} \tag{4}$$

is the CM of the mode $k = \text{a,s}$, $\varepsilon_l = \langle l_\text{s} l_\text{a}\rangle - \langle l_\text{s}\rangle\langle l_\text{a}\rangle$, $\delta_{l\bar{l}} = \langle l_\text{s}\bar{l}_\text{a}\rangle - \langle l_\text{s}\rangle\langle \bar{l}_\text{a}\rangle$ with $l,\bar{l} = q,p$ and $l \neq \bar{l}$. The matrix elements of $\boldsymbol{\sigma}_k$ can be directly measured from the homodyne traces of corresponding mode a_k (see Appendix A for further details), whereas the entries of $\boldsymbol{\sigma}_\delta$ cannot. However, the information about ε_l can be retrieved by changing the value of the mixer phase to $\Psi = \pm\pi/4$. In fact, it easy to show that [38–40] $\varepsilon_l = \frac{1}{2}(\langle l_+^2\rangle - \langle l_-^2\rangle) - \langle l_\text{s}\rangle\langle l_\text{a}\rangle$, $l = q,p$, where $q_\pm = X_0(t, \pm\pi/4|\Omega)$ and $p_\pm = X_{\pi/2}(t, \pm\pi/4|\Omega)$.

We now focus on $\delta_{l\bar{l}}$. Given the state ρ_Ω, but with different thermal contributions, these elements are equal to the energy unbalance between the sidebands (without the contribution due to the displacement that does not affect the CM),

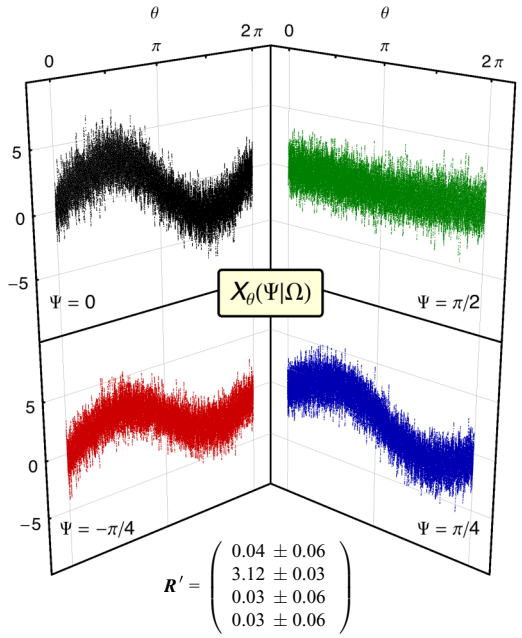

$$\boldsymbol{R}' = \begin{pmatrix} 0.04 \pm 0.06 \\ 3.12 \pm 0.03 \\ 0.03 \pm 0.06 \\ 0.03 \pm 0.06 \end{pmatrix}$$

$$\boldsymbol{\sigma}' = \begin{pmatrix} 1.00 \pm 0.03 & 0.1 \pm 0.1 & 0.04 \pm 0.09 & (0.1 \pm 0.1) \times 10^{-4} \\ & 1.03 \pm 0.3 & -(0.1 \pm 0.1) \times 10^{-4} & 0.0 \pm 0.2 \\ & & 1.01 \pm 0.01 & 0.0 \pm 0.02 \\ & & & 1.00 \pm 0.02 \end{pmatrix}$$

FIG. 2. Homodyne traces referring to the coherent two-mode sideband state and the reconstructed $\boldsymbol{R}'$ and $\boldsymbol{\sigma}'$. The purities of the modes $\mathcal{S}$ and $\mathcal{A}$ are $\mu_s = 0.99^{+0.01}_{-0.02}$ and $\mu_a = 0.99^{+0.01}_{-0.01}$, respectively. Only the relevant elements are shown.

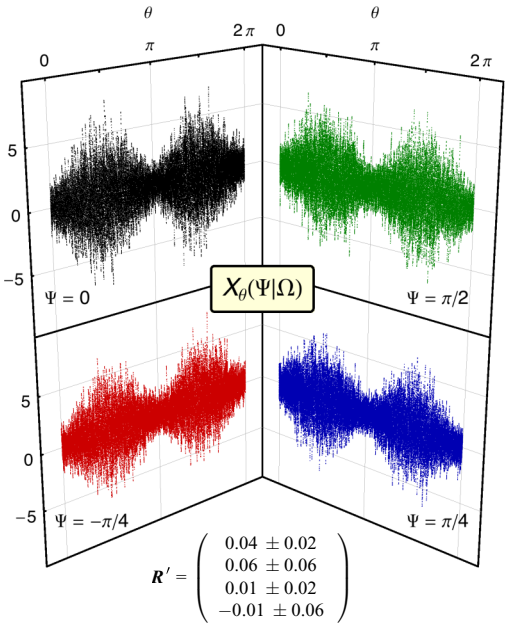

$$\boldsymbol{R}' = \begin{pmatrix} 0.04 \pm 0.02 \\ 0.06 \pm 0.06 \\ 0.01 \pm 0.02 \\ -0.01 \pm 0.06 \end{pmatrix}$$

$$\boldsymbol{\sigma}' = \begin{pmatrix} 0.50 \pm 0.03 & 0.03 \pm 0.06 & 0.02 \pm 0.08 & (0.1 \pm 0.1) \times 10^{-2} \\ & 4.2 \pm 0.2 & -(0.1 \pm 0.1) \times 10^{-2} & 0.02 \pm 0.07 \\ & & 0.49 \pm 0.03 & 0.03 \pm 0.05 \\ & & & 4.2 \pm 0.2 \end{pmatrix}$$

FIG. 3. Homodyne traces referring to the squeezed two-mode sideband state and the reconstructed $\boldsymbol{R}'$ and $\boldsymbol{\sigma}'$. The noise reduction is 3.1 ± 0.3 dB for both the modes $\mathcal{S}$ and $\mathcal{A}$, whereas their purities are $\mu_s = 0.68 \pm 0.07$ and $\mu_a = 0.67 \pm 0.02$, respectively. Only the relevant elements are shown.

namely, $\delta_{qp} = -\delta_{pq} = \Delta N_\Omega = (N_{+\Omega} - N_{-\Omega})$, as shown in Appendix A, and cannot be directly accessed by the spectral homodyne detection alone. To overcome this issue, a resonator detection method has been proposed and demonstrated in Refs. [29,32]. In our case we can exploit the error signal from the PDH stabilization to check the symmetry of the sideband state and also to measure the presence of some energy unbalance of the two sidebands, leading to nonvanishing $\delta_{l\bar{l}}$. More in details, as described in Appendix B, given the cavity bandwidth, the PDH error signal allows us to measure the unbalance as $\Delta N_\Omega = (\tau_{+\Omega} - \tau_{-\Omega})N_\Omega$, where $\tau_{\pm\Omega}$ are the relative transmission coefficients associated with the two sideband modes and $N_\Omega = N_{+\Omega} + N_{-\Omega}$ can be obtained from the (reconstructed) diagonal elements of $\boldsymbol{\sigma}_s$ and $\boldsymbol{\sigma}_a$ (see Appendix B) [41].

III. EXPERIMENTAL RESULTS

Given the state ρ_Ω, the full reconstruction of the CM requires the measurement of the quadratures of modes a_s,a_a, and $a_\pm = b(t, \pm\pi/4|\Omega)$. Once the mode has been selected by choosing the suitable mixer phase Ψ, the LO phase θ is scanned from 0 to 2π to acquire the corresponding homodyne trace. The statistical analysis of each trace allows us to reconstruct the expectation value of the moments of the quadrature required to reconstruct the CM $\boldsymbol{\sigma}'$ and the first moments vector $\boldsymbol{R}'$.

Figures 2, 3, and 4 show the experimental spectral homodyne traces corresponding to the coherent, squeezed, and squeezed-coherent two-mode sideband states, respectively. The coherent state is generated by removing the OPO pump and sending to the PMa (see Fig. 1) a sinusoidal signal at 3 MHz with the proper voltage amplitude in order to generate the desired number of photons on the sidebands. For the squeezed states, the OPO pump is set at ∼300 mW (well below the OPO threshold, which is about 4 times greater) whereas the input of the PMa seed generator is left in the vacuum (squeezed state) or modulated as in the case of the coherent state generation (squeezed-coherent state). As one can see, in the presence of squeezing (Figs. 3 and 4), all four traces exhibit a phase-dependent quadrature variance; the dependence disappears when the coherent two-mode sideband state is considered (Fig. 2). In this last case we can also see that for $\Psi = \pi/2$ the homodyne trace is that of the vacuum state, as one may expect. In the same figures we report the corresponding $\boldsymbol{\sigma}'$ and $\boldsymbol{R}'$. All the reconstructed $\boldsymbol{\sigma}'$ satisfy the physical condition $\boldsymbol{\sigma}' + i\boldsymbol{\Omega} \geqslant 0$ where $\boldsymbol{\Omega} = i\boldsymbol{\sigma}_y \oplus \boldsymbol{\sigma}_y$, $\boldsymbol{\sigma}_y$ being the Pauli matrix [36]. This implies that the modes $\mathcal{S}$ and $\mathcal{A}$ represent the same local quantum state, namely, $\boldsymbol{\sigma}_s = \boldsymbol{\sigma}_a$: this is in agreement with our measurement within statistical errors, as one can check from the Figs. 2–4. Furthermore, the diagonal elements of the off-diagonal blocks are zero within their statistical errors, in agreement with the expectation for a factorized state of the two modes.

We should now calculate the corresponding CMs in the modal basis $\hat{a}_{+\Omega}$ and $\hat{a}_{-\Omega}$ of the upper and lower sidebands, respectively. Because of Eq. (2) we can write $\boldsymbol{\sigma}_\Omega = \boldsymbol{S}^T \boldsymbol{\sigma}' \boldsymbol{S}$

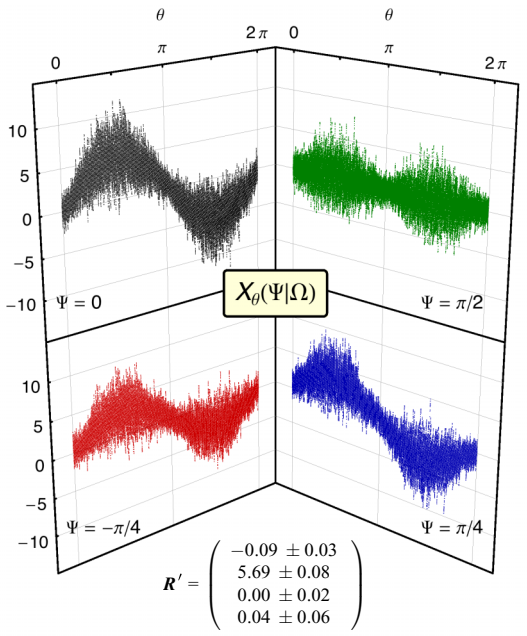

$$\boldsymbol{R}' = \begin{pmatrix} -0.09 \pm 0.03 \\ 5.69 \pm 0.08 \\ 0.00 \pm 0.02 \\ 0.04 \pm 0.06 \end{pmatrix}$$

$$\boldsymbol{\sigma}' = \begin{pmatrix} 0.53 \pm 0.04 & -0.1 \pm 0.2 & 0.02 \pm 0.03 & (0.1 \pm 0.1) \times 10^{-2} \\ & 4.1 \pm 0.2 & -(0.1 \pm 0.1) \times 10^{-2} & 0.2 \pm 0.4 \\ & & 0.57 \pm 0.03 & -0.09 \pm 0.05 \\ & & & 4.2 \pm 0.2 \end{pmatrix}$$

FIG. 4. Homodyne traces referring to the squeezed-coherent two-mode sideband state and the reconstructed $\boldsymbol{R}'$ and $\boldsymbol{\sigma}'$. The noise reduction is 2.7 ± 0.3 dB for the $\mathcal{S}$ mode and 2.4 ± 0.2 dB for the $\mathcal{S}$ mode, whereas the purities are $\mu_s = 0.68 \pm 0.07$ and $\mu_a = 0.64 \pm 0.02$, respectively. Only the relevant elements are shown.

and $\boldsymbol{R} = \boldsymbol{S}^T \boldsymbol{R}'$, where

$$\boldsymbol{S} = \frac{1}{\sqrt{2}} \begin{pmatrix} \mathbb{I} & \mathbb{I} \\ -i\boldsymbol{\sigma}_y & i\boldsymbol{\sigma}_y \end{pmatrix} \tag{5}$$

is the symplectic transformation associated with the mode transformations of Eq. (2). The results are summarized in Table I. Whereas the reconstructed two-mode sideband coherent state is indeed a product of two coherent states, the other two reconstructed states exhibit nonclassical features. In particular, the minimum symplectic eigenvalues of the corresponding partially transposed CMs [42,43] read $\tilde{\lambda} = 0.50 \pm 0.02$ and $\tilde{\lambda} = 0.55 \pm 0.03$ for the two-mode squeezed and squeezed-coherent state, respectively. Since in both cases $\tilde{\lambda} < 1$, we conclude that the sideband modes are entangled.

IV. CONCLUDING REMARKS

In conclusion, we have presented a measurement scheme to fully reconstruct the class of symmetric two-mode squeezed thermal states of spectral sideband modes from an optical parametric oscillator. This class of states, with Gaussian Wigner functions, is widely exploited in continuous-variable quantum technology. The scheme is based on homodyne detection and active stabilization, which guarantees phase coherence in every step of the experiment, and on a suitable analysis of the detected photocurrents. We have shown that by properly choosing the electronic mixer phase it is possible to select four different combinations of the upper and lower sidebands which, together with the information from the PDH error signal, allows us to reconstruct the elements of the covariance matrix of the state under consideration. The scheme has been successfully demonstrated to reconstruct both factorized and entangled sideband states.

In our implementation we used two electronic mixers and retrieved information about two modes at a time. It is also possible to use four mixers and extract information about four modes at the same time. The method is based on a single homodyne detector, the error signal from the active stabilization of the OPO, and does not involve elements outside the main detection tools of continuous-variable optical systems. As such, our procedure is indeed a versatile diagnostic tool, suitable to be embedded in quantum-information experiments with continuous-variable systems in the spectral domain, where, in particular, a state from an OPO is used as a signal or a quantum probe and, therefore, should be fully characterized.

TABLE I. Reconstructed first moment vectors $\boldsymbol{R}$ and CMs $\boldsymbol{\sigma}_\Omega$ of the two-mode sideband states ρ_Ω corresponding to the states of Figs. 2, 3 and 4, respectively.

- *Two-mode coherent state:*

$$R = (0.05 \pm 0.06,\ 2.18 \pm 0.05,\ 0.01 \pm 0.06,\ 2.23 \pm 0.05)^T$$

$$\sigma_\Omega = \begin{pmatrix} 1.00 \pm 0.02 & 0.0 \pm 0.1 & 0.00 \pm 0.02 & 0.1 \pm 0.1 \\ 0.0 \pm 0.1 & 1.02 \pm 0.02 & 0.0 \pm 0.1 & 0.01 \pm 0.02 \\ 0.00 \pm 0.02 & 0.0 \pm 0.1 & 1.00 \pm 0.02 & 0.0 \pm 0.1 \\ 0.1 \pm 0.1 & 0.01 \pm 0.02 & 0.0 \pm 0.1 & 1.02 \pm 0.02 \end{pmatrix}$$

- *Two-mode squeezed state:*

$$R = (0.02 \pm 0.04,\ 0.03 \pm 0.04,\ 0.03 \pm 0.04,\ 0.05 \pm 0.04)^T$$

$$\sigma_\Omega = \begin{pmatrix} 2.3 \pm 0.1 & 0.00 \pm 0.06 & -1.8 \pm 0.1 & 0.05 \pm 0.06 \\ 0.00 \pm 0.06 & 2.3 \pm 0.1 & 0.01 \pm 0.06 & 1.8 \pm 0.1 \\ -1.8 \pm 0.1 & 0.01 \pm 0.06 & 2.3 \pm 0.1 & 0.00 \pm 0.06 \\ 0.05 \pm 0.06 & 1.8 \pm 0.1 & 0.00 \pm 0.06 & 2.3 \pm 0.1 \end{pmatrix}$$

- *Two-mode squeezed-coherent state:*

$$R = (-0.09 \pm 0.05,\ 4.02 \pm 0.06,\ -0.03 \pm 0.05,\ 4.02 \pm 0.06)^T$$

$$\sigma_\Omega = \begin{pmatrix} 2.4 \pm 0.1 & 0.1 \pm 0.2 & -1.8 \pm 0.1 & 0.02 \pm 0.02 \\ 0.1 \pm 0.2 & 2.3 \pm 0.4 & 0.2 \pm 0.2 & 1.8 \pm 0.4 \\ -1.8 \pm 0.1 & 0.2 \pm 0.2 & 2.4 \pm 0.1 & -0.1 \pm 0.2 \\ 0.02 \pm 0.02 & 1.8 \pm 0.4 & -0.1 \pm 0.2 & 2.3 \pm 0.4 \end{pmatrix}$$

ACKNOWLEDGMENTS

M.G.A.P. and S.O. thank Alberto Porzio for useful discussions. This work was supported by UniMI through the UNIMI14 Grant No. 15-6-3008000-609 and the H2020 Transition Grant No. 15-6-3008000-625, and by the EU through the collaborative project QuProCS (Grant Agreement No. 641277).

APPENDIX A: COVARIANCE MATRIX ELEMENTS OF THE TWO-MODE SQUEEZED THERMAL STATE

In this Appendix we explicitly show how we can calculate the elements of the CM $\boldsymbol{\sigma}'$ given in Eq. (3). We recall that according to our definitions

$$b(t,0|\Omega) = \frac{\hat{a}_{+\Omega}(t) + \hat{a}_{-\Omega}(t)}{\sqrt{2}} \equiv a_{\rm s}, \tag{A1a}$$

$$b(t,\pi/2|\Omega) = i\,\frac{\hat{a}_{+\Omega}(t) - \hat{a}_{-\Omega}(t)}{\sqrt{2}} \equiv a_{\rm a}, \tag{A1b}$$

therefore the quadrature operator $X_\theta(t,\Psi|\Omega) = b(t,\Psi|\Omega)\,e^{-i\theta} + b^\dagger(t,\Psi|\Omega)\,e^{i\theta}$ can be written as

$$X_\theta(t,\Psi|\Omega) = \cos\Psi[q_s\cos\theta + p_s\sin\theta] + \sin\Psi[q_a\cos\theta + p_a\sin\theta].$$

If we set $\Psi = 0$, we have

$$X_0(t,0|\Omega) \equiv q_{\rm s} = a_{\rm s} + a_{\rm s}^\dagger = \frac{q_{+\Omega} + q_{-\Omega}}{\sqrt{2}} \Rightarrow \langle q_{\rm s}^2\rangle - \langle q_{\rm s}\rangle^2, \tag{A2a}$$

$$X_{\pi/2}(t,0|\Omega) \equiv p_{\rm s} = i(a_{\rm s}^\dagger - a_{\rm s}) = \frac{p_{+\Omega} + p_{-\Omega}}{\sqrt{2}} \Rightarrow \langle p_{\rm s}^2\rangle - \langle p_{\rm s}\rangle^2, \tag{A2b}$$

$$X_{\pm\pi/4}(t,0|\Omega) \equiv \frac{q_{\rm s} \pm p_{\rm s}}{\sqrt{2}} \Rightarrow \frac{1}{2}\langle q_{\rm s}p_{\rm s} + p_{\rm s}q_{\rm s}\rangle - \langle q_{\rm s}\rangle\langle p_{\rm s}\rangle, \tag{A2c}$$

and for $\Psi = \pi/2$ we obtain

$$X_0(t,\pi/2|\Omega) \equiv q_{\rm a} = a_{\rm a} + a_{\rm a}^\dagger = \frac{p_{-\Omega} - p_{+\Omega}}{\sqrt{2}} \Rightarrow \langle q_{\rm a}^2\rangle - \langle q_{\rm a}\rangle^2, \tag{A3a}$$

$$X_{\pi/2}(t,\pi/2|\Omega) \equiv p_{\rm a} = i(a_{\rm a}^\dagger - a_{\rm a}) = \frac{q_{+\Omega} - q_{-\Omega}}{\sqrt{2}} \Rightarrow \langle p_{\rm a}^2\rangle - \langle p_{\rm a}\rangle^2, \tag{A3b}$$

$$X_{\pm\pi/4}(t,\pi/2|\Omega) \equiv \frac{q_{\rm a} \pm p_{\rm a}}{\sqrt{2}} \Rightarrow \frac{1}{2}\langle q_{\rm a}p_{\rm a} + p_{\rm a}q_{\rm a}\rangle - \langle q_{\rm a}\rangle\langle p_{\rm a}\rangle, \tag{A3c}$$

On the other hand, if we set $\Psi = \pm\pi/4$ we find

$$X_0(t,\pm\pi/4|\Omega) = \frac{q_{\rm a} \pm q_{\rm s}}{\sqrt{2}},$$

$$X_{\pi/2}(t,\pm\pi/4|\Omega) = \frac{p_{\rm s} \pm p_{\rm a}}{\sqrt{2}},$$

and we have the following identities:

$$\left\langle X_0^2(t,\pi/4|\Omega) - X_0^2(t,-\pi/4|\Omega)\right\rangle = 2\langle q_{\rm a}q_{\rm s}\rangle \equiv \varepsilon_q, \tag{A4}$$

$$\left\langle X_{\pi/2}^2(t,\pi/4|\Omega) - X_{\pi/2}^2(t,-\pi/4|\Omega)\right\rangle = 2\langle p_{\rm a}p_{\rm s}\rangle \equiv \varepsilon_p. \tag{A5}$$

As mentioned in Sec. II, it is not possible to calculate the elements δ_{qp} and δ_{pq} directly from the spectral homodyne traces [29]. However, when the state under consideration is a two-mode squeezed thermal state $\rho_\Omega = D_2(\alpha)S_2(\xi)\nu_{+\Omega}(N_1)\otimes\nu_{-\Omega}(N_2)S_2^\dagger(\xi)D_2^\dagger(\alpha)$, where $D_2(\alpha) = \exp\{[\alpha(a_{+\Omega}^\dagger + a_{-\Omega}^\dagger) - \text{H.c.}]/\sqrt{2}\}$ is the symmetric displacement operator, $S_2(\alpha) = \exp(\xi a_{+\Omega}^\dagger a_{-\Omega}^\dagger - \text{H.c.})$ is the two-mode squeezing operator, and $\nu_{\pm\Omega}(N)$ is the thermal state of mode $a_{\pm\Omega}$ with N average photons [36], we can calculate δ_{qp} and δ_{pq} as follows.

Since the covariance matrix does not depend on the displacement operator, we can assume α. Furthermore, it is useful to introduce the following parametrization: we define the squeezed photons per mode $N_{\rm sq} = \sinh^2 r$, the total number of thermal photons $N_{\rm th} = N_1 + N_2$, and the thermal-photon fraction $R_{\rm th} = N_1/N_{\rm th}$. Thereafter, the energies of the two sidebands are given by

$$N_{+\Omega} = N_{\rm sq}(1 + N_{\rm th}) + R_{\rm th}N_{\rm th},$$
$$N_{-\Omega} = N_{\rm sq}(1 + N_{\rm th}) + (1 - R_{\rm th})N_{\rm th},$$

respectively, and thus

$$N_{+\Omega} + N_{-\Omega} = 2N_{\rm sq} + N_{\rm th}(1 + 2N_{\rm sq}),$$
$$N_{+\Omega} - N_{-\Omega} = N_{\rm th}(2R_{\rm th} - 1).$$

The covariance matrix associated with ρ_Ω has the following block-matrix form:

$$\boldsymbol{\sigma}_\Omega = \begin{pmatrix} A\,\mathbb{I} & C\,\boldsymbol{\sigma}_z \\ C\,\boldsymbol{\sigma}_z & B\,\mathbb{I} \end{pmatrix}, \tag{A6}$$

where $\boldsymbol{\sigma}_z$ is the Pauli matrix and

$$A = 1 + 2N_{\rm sq}(1 + N_{\rm th}) + 2R_{\rm th}N_{\rm sq},$$
$$B = 1 + 2N_{\rm sq}(1 + N_{\rm th}) + 2(1 - R_{\rm th})N_{\rm sq},$$
$$C = 2(1 + N_{\rm th})\sqrt{N_{\rm sq}(1 + N_{\rm sq})}.$$

The corresponding *measured* covariance matrix reads

$$\boldsymbol{\sigma}' = \begin{pmatrix} \frac{1}{2}(A + B)\,\mathbb{I} + C\,\boldsymbol{\sigma}_z & (N_{+\Omega} - N_{-\Omega})\,i\boldsymbol{\sigma}_y \\ N_{+\Omega} - N_{-\Omega})\,i\boldsymbol{\sigma}_y & \frac{1}{2}(A + B)\,\mathbb{I} + C\,\boldsymbol{\sigma}_z \end{pmatrix}, \tag{A7}$$

$\boldsymbol{\sigma}_y$ being the Pauli matrix. Note that while $\boldsymbol{\sigma}'$ is always symmetric, $\boldsymbol{\sigma}_\Omega$ can be also asymmetric.

APPENDIX B: RETRIEVING THE ENERGY UNBALANCE OF THE TWO-MODE SQUEEZED THERMAL STATE

In our setup, the presence of the energy unbalance between the sidebands is due to the possible difference between the cavity transmission coefficients of the involved modes. Therefore, to determine the energy unbalance, we measure the normalized OPO cavity transmission coefficient when resonant with the pump, its bandwidth $\Delta\omega$ and get the corresponding analytical fit $T_0(\omega)$. Then, we consider the error signal $E_{\rm PDH}(\delta x)$ of the PDH [34], where $\delta x = L - L_0$, L and L_0 being the actual

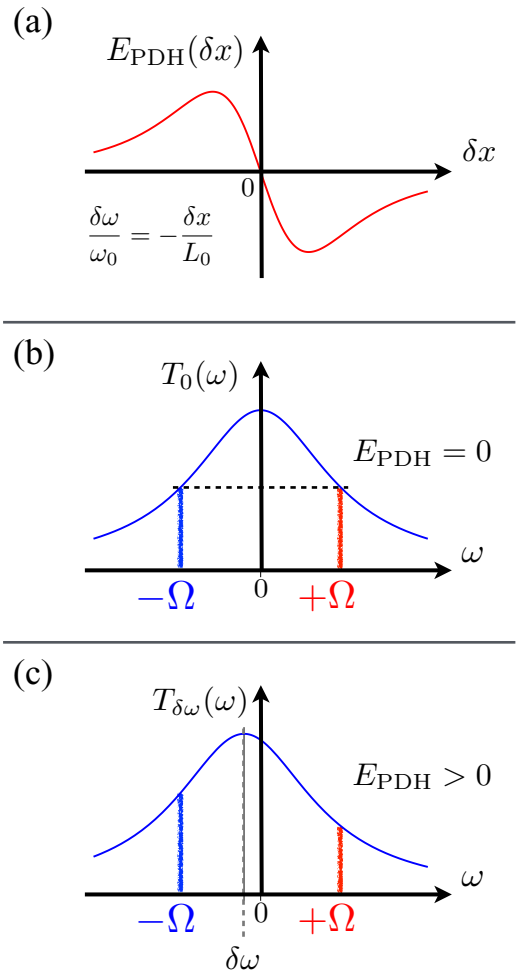

FIG. 5. (a) PDH error signal as function of the cavity displacement $\delta x = L - L_0$, where L is the cavity length and L_0 refers to the resonant condition with the pump at ω_0: the value of $E_{\rm PDH}$ allows us to retrieve the information about the detuning $\delta\omega$. (b) Cavity transmission coefficient as a function of ω when $E_{\rm PDH} = 0$; one has the maximum $T_0(0) = 1$ and $T_0(+\Omega) = T_0(-\Omega)$. (b) Cavity transmission coefficient as a function of ω in the presence $E_{\rm PDH} \neq 0$ (in the plot we consider $E_{\rm PDH} > 0$); now one finds the transmissivity maximum at $\delta\omega$, namely, $T_{\delta\omega}(\delta\omega) = 1$. Note that $T_{\delta\omega}(\omega) = T_0(\omega - \delta\omega)$ and it is clear that $T_{\delta\omega}(+\Omega) \neq T_{\delta\omega}(-\Omega)$. Starting from the measured $E_{\rm PDH}(\delta x)$, one can retrieve the value $\delta\omega$ and, thereafter, the sideband transmission coefficients $T_{\delta\omega}(+\Omega)$ and $T_{\delta\omega}(-\Omega)$. For the sake of clarity we did not report the real experimental signals, but their pictorial view to better explain our analysis. See the text for details.

cavity length and its length at resonance with the pump, respectively, see Fig. 5(a). The detuning is thus given by $\delta\omega = -\omega_0\,\delta x/L_0$. If $|\delta\omega| \ll \Delta\omega$, which is our working regime, we can expand the error signal as $E_{\rm PDH}(\delta x) \approx \kappa\,\delta x$, where we used $E_{\rm PDH}(0) = 0$ and $\kappa = \partial_{\delta x} E_{\rm PDH}(0)$ is directly measured from the experimental PDH signal. At resonance, the cavity has a maximum of the (normalized) transmissivity at $\omega = 0$ (or $L = L_0$) and the corresponding PDH error signal vanishes, namely, $E_{\rm PDH}(0) = 0$. This scenario is sketched in Fig. 5(b), where we show a pictorial view of $T_0(\omega)$ when $E_{\rm PDH} = 0$: we have that $T_0 = 1$ and, thus, due to the symmetry of $T_0(\omega)$, we find $T_0(+\Omega) = T_0(-\Omega)$. In the presence of a detuning $|\delta\omega| \ll \Delta\omega$, we measure a PDH error signal $E^{(\rm exp)}_{\rm PDH} = E_{\rm PDH}(\delta x) \neq 0$, see Fig. 5(c) (note that now the maximum of the transmissivity is reached at $\omega = \delta\omega$). Therefore, we can retrieve the actual value of detuning as $\delta\omega = -\omega_0\,E^{(\rm exp)}_{\rm PDH}/(\kappa\,L_0)$ and use it to obtain the information about the (normalized) sideband transmission coefficients $T_{\delta\omega}(+\Omega)$ and $T_{\delta\omega}(-\Omega)$ starting from $T_{\delta\omega}(\omega) = T_0(\omega - \delta\omega)$. Eventually, we can assess the relative cavity transmission coefficients

$$\tau_{\pm\Omega} = \frac{T_{\delta\omega}(\pm\Omega)}{T_{\delta\omega}(+\Omega) + T_{\delta\omega}(-\Omega)}, \tag{B1}$$

associated with the two sideband modes, and the energy difference can be obtained as

$$N_{+\Omega} - N_{-\Omega} = \frac{T_{\delta\omega}(+\Omega) - T_{\delta\omega}(-\Omega)}{T_{\delta\omega}(+\Omega) + T_{\delta\omega}(-\Omega)}\,(N_{+\Omega} + N_{-\Omega}). \tag{B2}$$

In general, given the covariance matrix $\boldsymbol{\sigma}$ of a Gaussian state, the total energy can be obtained from the sum of its diagonal elements $[\boldsymbol{\sigma}]_{kk}$ as (without loss of generality we are still assuming the absence of the displacement)

$$N_{\rm tot} = \frac{1}{4}\sum_{k=1}^{4}[\boldsymbol{\sigma}]_{kk} - 1. \tag{B3}$$

Experimentally, we can find the total energy $N_{+\Omega} + N_{-\Omega}$ from the first and second moments of the operators in Eqs. (A2) and (A3), which are measured from the homodyne detection.

[1] A. I. Lvovsky, H. Hansen, T. Aichele, O. Benson, J. Mlynek, and S. Schiller, Phys. Rev. Lett. **87**, 050402 (2001).
[2] A. Zavatta, M. Bellini, P. L. Ramazza, F. Marin, and F. T. Arecchi, J. Opt. Soc. Am. B **19**, 1189 (2002).
[3] A. I. Lvovsky and J. H. Shapiro, Phys. Rev. A **65**, 033830 (2002).
[4] S. A. Babichev, B. Brezger, and A. I. Lvovsky, Phys. Rev. Lett. **92**, 047903 (2004).
[5] A. Zavatta, S. Viciani, and M. Bellini, Phys. Rev. A **70**, 053821 (2004).
[6] A. Zavatta, S. Viciani, and M. Bellini, Science **306**, 660 (2004).
[7] V. Parigi, A. Zavatta, M. S. Kim, and M. Bellini, Science **317**, 1890 (2007).
[8] S. Grandi, A. Zavatta, M. Bellini, and M. G. A. Paris, arXiv:1505.03297 [quant-ph].
[9] E. Jakeman, C. J. Oliver, and E. R. Pike, Adv. Phys. **24**, 349 (1975).
[10] H. P. Yuen and W. S. Chan, Opt. Lett. **8**, 177 (1983).
[11] B. L. Schumaker, Opt. Lett. **9**, 189 (1984).

[12] G. L. Abbas, V. W. S. Chan, and S. T. Yee, Opt. Lett. **8**, 419 (1983).
[13] B. Yurke, Phys. Rev. A **32**, 300 (1985).
[14] D. T. Smithey, M. Beck, M. G. Raymer, and A. Faridani, Phys. Rev. Lett. **70**, 1244 (1993).
[15] M. G. Raymer, M. Beck, and D. F. McAlister, Phys. Rev. Lett. **72**, 1137 (1994).
[16] D. T. Smithey, M. Beck, J. Cooper, and M. G. Raymer, Phys. Rev. A **48**, 3159 (1993).
[17] K. Vogel and H. Risken, Phys. Rev. A **40**, 2847 (1989).
[18] G. M. D'Ariano, C. Macchiavello, and M. G. A. Paris, Phys. Rev. A **50**, 4298 (1994).
[19] M. Munroe, D. Boggavarapu, M. E. Anderson, and M. G. Raymer, Phys. Rev. A **52**, R924 (1995).
[20] S. Schiller, G. Breitenbach, S. F. Pereira, T. Muller, and J. Mlynek, Phys. Rev. Lett. **77**, 2933 (1996).
[21] G. Breitenbach, S. Schiller, and J. Mlynek, Nature **387**, 471 (1997).
[22] G. M. D'Ariano, M. G. A. Paris, and M. F. Sacchi, Adv. Imaging Electron Phys. **128**, 205 (2003).
[23] A. I. Lvovsky and M. G. Raymer, Rev. Mod. Phys. **81**, 299 (2009).
[24] M. Gu, H. M. Chrzanowski, S. M. Assad, T. Symul, K. Modi, T. C. Ralph, V. Vedral, and P. K. Lam, Nat. Phys. **8**, 671 (2012).
[25] L. S. Madsen, A. Berni, M. Lassen, and U. L. Andersen, Phys. Rev. Lett. **109**, 030402 (2012).
[26] R. Blandino, M. G. Genoni, J. Etesse, M. Barbieri, M. G. A. Paris, P. Grangier, and R. Tualle-Brouri, Phys. Rev. Lett. **109**, 180402 (2012).
[27] C. Peuntinger, V. Chille, L. Mista Jr., N. Korolkova, M. Förtsch, J. Korger, C. Marquardt, and G. Leuchs, Phys. Rev. Lett. **111**, 230506 (2013).
[28] V. Chille, N. Quinn, C. Peuntinger, C. Croal, L. Mista, Jr., C. Marquardt, G. Leuchs, and N. Korolkova, Phys. Rev. A **91**, 050301(R) (2015).
[29] F. A. S. Barbosa, A. S. Coelho, K. N. Cassemiro, P. Nussenzveig, C. Fabre, A. S. Villar, and M. Martinelli, Phys. Rev. A **88**, 052113 (2013).
[30] E. H. Huntington, G. N. Milford, C. Robilliard, T. C. Ralph, O. Glöckl, U. L. Andersen, S. Lorenz, and G. Leuchs, Phys. Rev. A **71**, 041802(R) (2005).
[31] E. H. Huntington and T. C. Ralph, J. Opt. B **4**, 123 (2002).
[32] F. A. S. Barbosa, A. S. Coelho, K. N. Cassemiro, P. Nussenzveig, C. Fabre, M. Martinelli, and A. S. Villar, Phys. Rev. Lett. **111**, 200402 (2013).
[33] K. Somiya, Phys. Rev. D **67**, 122001 (2003).
[34] R. W. P. Drever, J. L. Hall, F. V. Kowalski, J. Hough, G. M. Ford, A. J. Munley, and H. Ward, Appl. Phys. B **31**, 97 (1983).
[35] H.-A. Bachor and T. C. Ralph, *A Guide to Experiments in Quantum Optics* (Wiley, New York, 2004).
[36] S. Olivares, Eur. Phys. J. ST **203**, 3 (2012).
[37] C. Weedbrook, S. Pirandola, R. Garcia-Patrón, N. J. Cerf, T. C. Ralph, J. H. Shapiro, and S. Lloyd, Rev. Mod. Phys. **84**, 621 (2012).
[38] V. D'Auria, A. Porzio, S. Solimeno, S. Olivares, and M. G. A. Paris, J. Opt. B **7**, S750 (2005).
[39] V. D'Auria, S. Fornaro, A. Porzio, S. Solimeno, S. Olivares, and M. G. A. Paris, Phys. Rev. Lett. **102**, 020502 (2009).
[40] D. Buono, G. Nocerino, V. D'Auria, A. Porzio, S. Olivares, and M. G. A. Paris, J. Opt. Soc. Am. B **27**, A110 (2010).
[41] A. Ferraro, S. Olivares, and M. G. A. Paris, *Gaussian States in Quantum Information* (Bibliopolis, Naples, Italy, 2005).
[42] R. Simon, Phys. Rev. Lett. **84**, 2726 (2000).
[43] A. Serafini, F. Illuminati, and S. De Siena, J. Phys. B **37**, L21 (2004).